ACS Synthetic Biology

Letter

NADPH-auxotrophic E. coli: a sensor strain for testing in vivo regeneration of NADPH

Steffen N. Lindner, Liliana Calzadíaz Ramirez, Jan Krüsemann, Oren Yishai, Sophia Belkhelfa, Hai He, Madeleine Bouzon, Volker Döring, and Arren Bar-Even

ACS Synth. Biol., **Just Accepted Manuscript** • DOI: 10.1021/acssynbio.8b00313 • Publication Date (Web): 26 Nov 2018

ACS Publications

is published by the American Chemical Society. 1155 Sixteenth Street N.W., Washington, DC 20036

NADPH-auxotrophic *E. coli*: a sensor strain for testing *in vivo* regeneration of NADPH

Steffen N. Lindner†*, Liliana Calzadiaz Ramirez†, Jan Krüsemann†, Oren Yishai†, Sophia Belkhelfa‡, Hai He†, Madeleine Bouzon‡, Volker Döring‡, Arren Bar-Even†*

†Max Planck Institute of Molecular Plant Physiology, Am Mühlenberg 1, 14476 Potsdam-Golm, Germany

‡Génomique Métabolique, Genoscope, Institut François Jacob, CEA, CNRS, Univ Evry, Université Paris-Saclay, 91057 Evry, France

* corresponding authors:

Steffen N. Lindner

Phone: +49 331 567-8910

Email: Lindner@mpimp-golm.mpg.de

Arren Bar-Even

Phone: +49 331 567-8910

Email: Bar-Even@mpimp-golm.mpg.de

Key words: NADPH regeneration; auxotroph strain; selection strain; enzyme screening; dihydrolipoamide dehydrogenase; glyceraldehyde 3-phosphate dehydrogenase; formate dehydrogenase; cinnamyl alcohol.

Abstract

Insufficient rate of NADPH regeneration often limits the activity of biosynthetic pathways. Expression of NADPH-regenerating enzymes is commonly used to address this problem and increase cofactor availability. Here, we construct an *Escherichia coli* NADPH-auxotroph strain, which is deleted in all reactions that produce NADPH with the exception of 6-phosphogluconate dehydrogenase. This strain grows on a minimal medium only if gluconate is added as NADPH source. When gluconate is omitted, the strain serves as a 'biosensor' for the capability of enzymes to regenerate NADPH *in vivo*. We show that the NADPH-auxotroph strain can be used to quantitatively assess different NADPH-regenerating enzymes and provide essential information on expression levels and/or concentrations of reduced substrates required to support optimal NADPH production rate. The NADPH-auxotroph strain thus provides a fast and effective metabolic platform for evaluating NADPH regeneration within the cellular context.

NADPH is the main electron donor for anabolic pathways and serves as a primary driving force in the biosynthesis of a wide array of value added chemicals. However, in many cases, the endogenous rate of NADPH regeneration does not suffice to support the production of chemicals whose biosynthesis requires high stoichiometric amounts of this cofactor, e.g., lysine[1], valine[2], arginine[3], ornithine[4], chloropropionate[5], lycopene[5], and terpenoids[6]. Several strategies are used to overcome this limitation[7-10]. One approach is to divert metabolic flux towards endogenous pathways that produce NADPH, e.g., the oxidative pentose phosphate pathway. Alternatively, heterologous overexpression of NADP-dependent oxidoreductase enzymes can enhance cofactor regeneration. This latter strategy is also used in *in vitro* biosynthesis systems, where NADPH is regenerated by the addition of a reduced compound which can donate its electrons to $NADP^+$ via an appropriate enzyme[11]. In some cases, NADH-regenerating enzymes are engineered to accept $NADP^+$, e.g., formate dehydrogenase[12], phosphite dehydrogenase[13].

Here, we construct an NADPH-auxotrophic *E. coli* strain, deleted in all endogenous NADPH-producing reactions, with the exception of 6-phosphogluconate dehydrogenase. This strain can grow on a minimal medium only if supplemented with gluconate as sole source of NADPH regeneration. We show that this strain can serve as an efficient 'metabolic biosensor' for the ability of different enzymes to regenerate NADPH *in vivo*, providing valuable information on the required expression levels and the optimal concentrations of electron donors. This strain could therefore serve as a useful metabolic platform to compare different strategies of NADPH regeneration, further enabling direct screening of oxidoreductase enzymes for high NADPH production rate.

Results

Construction and characterization of a NADPH auxotroph strain

E. coli harbors five enzymes that regenerate NADPH. These are glucose 6-phosphate dehydrogenase (Zwf) and 6-phosphogluconate dehydrogenase (Gnd) of the oxidative pentose phosphate pathway, a malic enzyme (MaeB), isocitrate dehydrogenase (Icd) of the TCA cycle, and a membrane-bound proton-translocating transhydrogenase (PntAB)[14]. To create an NADPH-auxotroph strain, we aimed to delete all of these enzymes with the exception of Gnd. As the activity of Gnd depends on the availability of 6-phosphogluconate, disruption of Zwf would deprive the former enzyme from its substrate, rendering it incapable of regenerating NADPH from glucose 6-phosphate (Figure 1). The advantage of this design is that the addition of gluconate serves as a 'relaxing substrate': as the conversion of gluconate to 6-phosphogluconate is independent of the activity of Zwf, this substrate would support NADPH-regeneration by Gnd (Figure 1).

Figure 2 presents the growth phenotypes of intermediate gene deletion strains that were constructed towards a NADPH auxotrophic phenotype. Disruption of Zwf and MaeB (abbreviated by 'Z' and 'M' in Figure 2) did not alter growth on any of the carbon sources tested (Figure 2A, concentrations of feedstocks were normalized according to their energies of combustion, see Methods). However, further disruption of PntAB (abbreviated by 'P') severely inhibited growth on gluconate and abolished growth on most other carbon sources, despite the availability of Icd as a NADPH source (Figure 2B). Only growth on acetate remained unperturbed, presumably as acetate oxidation via the TCA cycle produces NADPH at high rate via Icd. We speculated that the growth defect observed with most carbon sources can be explained by the activity of the soluble transhydrogenase (SthA) which depletes the NADPH pool by transferring electrons to NAD^+.[14] Indeed, as shown in Figure 2C, upon further disruption of

SthA (abbreviated by 'S'), growth on all carbon sources, except of glucose, was restored (the very poor growth on glucose cannot be easily explained but might be related to the vast regulatory effects induced by this carbon source).

Next, we integrated the above gene deletions with the disruption of Icd, a key enzyme of the TCA cycle. As reported before[15], we found that knockout of the isocitrate dehydrogenase gene reduced growth rate and further required the addition of 2-ketoglutarate – the endogenous product of Icd – as precursor of glutamate and downstream amino-acids. When combined with the deletion of *zwf* and *maeB*, disruption of Icd (abbreviated by 'I') resulted in severely impaired growth – considerably worse than that of the Δ*icd* strain alone – with all carbon sources besides the 'relaxing' substrate gluconate (Figure 2D). This points to the prime role of Icd for the regeneration of NADPH when Zwf and MaeB are not available. Deletion of *zwf*, *maeB*, *icd*, and *pntAB* completely abolished growth in a minimal medium on all carbon sources (Figure 2E). Yet, further disruption of SthA restored growth on gluconate (Figure 2F), pointing again to the role of SthA in depleting the NADPH pool. This final strain NADPHaux (Δ*zwf* Δ*maeB* Δ*icd* Δ*pntAB* Δ*sthA*) therefore presents the desired growth phenotype, i.e., growing only when the 'relaxing' substrate gluconate is available.

Next, we tested whether addition of small amounts of gluconate rescue the growth of the NADPHaux strain on different carbon sources. As shown in Figure 3, the concentration of added gluconate directly correlates with the final OD reached when cells were grown on multiple carbon sources. We further deleted phosphogluconate dehydratase (Edd) and 2-keto-3-deoxygluconate 6-phosphate aldolase (Eda) of the Entner-Doudoroff pathway, which competes with Gnd on the substrate 6-phosphogluconate. Yet, as demonstrated in Figure 3, the effect of this deletion was relatively small, with several few expectations. This indicates that under most conditions, in our gene-deletion strain, the majority of 6-phosphogluconate is metabolized via Gnd rather than the Entner-Doudoroff pathway.

The NADPHaux strain enables direct selection for NADPH production by different enzymes and reduced substrates

To test whether the NADPHaux strain could be used to evaluate the capability of different enzymes to regenerate NADPH, we used several NADP-dependent oxidoreductases. We started with a dihydrolipoamide dehydrogenase from *E. coli* – a key component of the pyruvate and 2-ketoglutarate dehydrogenase complexes, as well of the glycine cleavage system – that was engineered to prefer the reduction of $NADP^+$ over NAD^+ [16]. This engineered enzyme displays very good kinetics of $NADP^+$, having k_{cat} = 95.2 sec^{-1} and K_M = 60 μM, which are considerably better than the average enzyme[17]. Indeed, as shown in Figure 4, when we expressed the enzyme from a medium copy number plasmid (p15A origin of replication) and under the regulation of a medium strength promoter (variant 10 of *pgi*-promoter[18-19]), we observed stable growth on all tested carbon sources – with the exception of acetate – indicating high production rate of NADPH.

The failure to establish growth on acetate, as well as the poor growth we observe on pyruvate and succinate can be related to the operation of the PEP-glyoxylate cycle in our strain, in which the TCA cycle is disrupted[20]. Specifically, this cycle – which relies on the glyoxylate shunt, the malic enzyme, and pyruvate dehydrogenase – can replace the TCA cycle and support complete oxidation of carbon feedstocks[20]. Growth on carbon sources that enter 'lower' metabolism, i.e., acetate, pyruvate, and succinate, are expected to heavily rely on the activity

of this alternative cycle for energy production. Excess $NADP^+$ reduction by pyruvate dehydrogenase (carrying the mutated dihydrolipoamide dehydrogenase) could inhibit the operation of this cycle and hence result in poor or no growth on carbon sources that enter 'lower' metabolism.

Next, we tested the NADP-dependent non-phosphorylating glyceraldehyde 3-phosphate dehydrogenase (GapN) of *Streptococcus mutans*[21]. This enzyme irreversibly oxidizes glyceraldehyde 3-phosphate to 3-phosphoglycerate using $NADP^+$ as an electron acceptor. GapN was previously demonstrated to enhance NADPH regeneration[22], and its kinetic parameters with $NADP^+$ are good: k_{cat} = 60 sec^{-1} and K_M = 25 μM[23]. Yet, overexpression of the enzyme from a medium copy number plasmid and under the regulation of a medium strength promoter resulted in only poor growth. Only when we replaced the medium strength promoter with a strong promoter (variant 20 of *pgi*-promoter[18-19]) – increasing expression level ~3 fold[19] – we observed good growth on all carbon sources, as shown in Figure 5A.

Notably, growth on carbon sources that enter 'lower' metabolism required a cyclic flux between 3-phosphoglycerate and glyceraldehyde 3-phosphate to produce NADPH, or, more accurately, to transfer electrons from NADH to $NADP^+$. As shown schematically in Figure 5B, this transfer of reducing power comes at the expense of ATP hydrolysis (by the combined activity of 3-phosphoglycerate kinase and glyceraldehyde 3-phosphate dehydrogenase), and thus mimics the activity of PntAB that uses the proton motive force to energize this reaction. This cycle further resembles an endogenous NADPH regeneration cycle – composed of PEP synthetase, PEP carboxylase, oxaloacetate dehydrogenase, and the NADPH-generating malic enzyme (MaeB)[24] – the latter being deleted in the NADPHaux strain.

We then tested a previously reported formate dehydrogenase (FDH) from *Mycobacterium vaccae* N10 that was engineered, and demonstrated *in vitro*, to prefer the reduction of $NADP^+$ [25]. Yet, the kinetic parameters of the enzyme with $NADP^+$ are quite poor – k_{cat} = 3.1 sec^{-1} and K_M = 147 μM. Indeed, overexpression of the enzyme from a medium copy number plasmid failed to sustain growth upon addition of formate, regardless of the promoter used. Only when we expressed the enzyme from a high copy number plasmid (pMB1 origin of replication; under a medium strength promoter, equivalent to a ~6-fold higher expression level compared to a medium copy number plasmid[19]), we could sustain stable formate-dependent growth. As shown in figure 6, increasing formate concentration up to 30 mM resulted in an increased growth rate, which can be explained by the very high K_M of the enzyme for formate[25]. Concentrations higher than 30 mM did not improve growth, suggesting that the enzyme operates near saturation. (We note that the intracellular formate concentration is not expected to differ substantially from its concentration in the medium as this small molecule can easily diffuse into the cell, which is further assisted by the formate channel focA[26].)

Finally, we tested the ability of *E. coli* to endogenously use different reduced compounds to regenerate NADPH, without introducing new enzymes. We tested several alcohols and found one compound that can be natively used to produce NADPH: cinnamyl alcohol. As shown in Figure 7, a concentration as low as 0.25 mM of cinnamyl alcohol sufficed to support growth, albeit at a low rate. 4 mM of cinnamyl alcohol was optimal to support growth, where higher concentrations resulted in a decreased growth rate, probably due to the toxicity of the compound. These results suggest that cinnamyl alcohol is oxidized to cinnamic acid by endogenous, promiscuous alcohol and aldehyde dehydrogenases, of which at least one regenerates NADPH. Oxidation to cinnamaldehyde without

further oxidation to cinnamic acid is unlikely, as the oxidation of an alcohol to aldehyde is unfavorable and would not to be efficient at such low a concentration of the alcohol substrate.

Discussion

The intermediate deletion strains, constructed *en route* to the NADPHaux strain, present interesting behavior that indicates how NADPH levels are balanced *in vivo*. Specifically, the growth retardation associated with the strains deleted in *pntAB* but not in *sthA* (Figure 2B, E) suggests that rather than being expressed only when necessary, these metabolically counteracting systems operate in parallel. Hence, when PntAB is absent (together with Zwf and MaeB) the cell does not deactivate SthA, which leads to a deleterious depletion of the NADPH pool. This finding fits previous reports showing that the regulation of the two transhydrogenases is independent of the actual availability of NADPH and rather corresponds to nutrient levels and growth rate[27]. While it was proposed that *sthA* might be allosterically activated with NADPH and inhibited by $NADP^+$ [14], it seems that this effect does not suffice to prevent the depletion of the NADPH pool by *sthA* (at least in our NADPH-starved strains).

The simultaneous activities of PntAB and SthA suggest the existence of a futile cycle, where NADH is converted to NADPH just to be recycled back to NADH, at the expense of proton relocation that dissipates about a third of the energy of the hydrolysis of one ATP molecule. While this futile cycle might be costly in terms of cellular resources, it could have an important regulatory function, enabling a fast balancing of the levels of NADPH under changing conditions.

Using several examples, we illustrated the applicability of the NADPHaux strain to detect $NADP^+$ reduction activity. Importantly, we demonstrated that the strain can accurately sense the rate of NADPH regeneration, such that enzymes with superior kinetics can be expressed at moderate levels while enzymes characterized by poor kinetics require high expression level to support growth. Our system is therefore useful to quantitatively decipher the suitability of different enzymes to regenerate NADPH and to further suggest appropriate expression levels to efficiently support this activity. Moreover, as we show with the case of formate and cinnamyl alcohol, the NADPHaux strain is useful to quantitatively elucidate the required concentration of an electron donor to support a maximal regeneration rate.

Our findings with regards to NADPH regeneration by formate and FDH is especially interesting in the context of the 'formate bioeconomy', i.e., using formate – produced via physicochemical means, e.g., electrochemical reduction of CO_2 – as feedstock for microbial growth and bioproduction[28]. Specifically, most formatotrophic organisms transfer electrons from formate to NAD^+ to provide reducing power and energy for growth. As some formate assimilation pathways require high NADPH input – for example, reduction of 5,10-methenyltetrahydrofolate within the reductive glycine pathway[29] – the transfer of reducing power from NADH to $NADP^+$, e.g., by the activity of PntAB, can dissipate a substantial fraction of cellular energy. Expressing a NADP-dependent formate dehydrogenase, which directly transfers reducing power from formate to $NADP^+$, would therefore provide an energy efficient alternative that could boost biomass and bioproduction yields.

The NADPHaux strain is a simple but effective tool to support enzyme engineering and the successful realization of diverse biosynthetic pathways using a simple growth/no-growth readout. This strain would be especially useful

for the testing large libraries of enzyme variants: instead of time-consuming screening of each variant for its ability to reduce $NADP^+$ at a sufficient rate, the entire library can be transformed to the NADPHaux strain, and the highly active enzymes isolated from the (fast) growing cells.

Materials and Methods

Strains and gene deletions

The strains used in this study are listed in Table 1. *E. coli* strain SIJ488[30], was used as WT for the sequential deletion of genes. SIJ488 genomically carries inducible genes that encode for a recombinase and a flippase, allowing fast turnover for multiple deletions. Most gene deletions were performed by successive rounds of λ-Red recombineering [30]. The gene *icd* was deleted by P1 phage transduction [31] using the *icd* knock out strain from the Keio collection (Table 1) as a donor [32].

For the recombination, kanamycin resistance cassettes were generated via PCR – 'KO' primers with 50 bp homologous arms are listed in Supplementary Table 1 – using the FRT-PGK-gb2-neo-FRT (Km) cassette (Gene Bridges, Germany). To prepare cells for gene deletion, fresh cultures were inoculated in LB in the morning and the recombinase genes were induced by addition of 15 mM L-arabinose at OD ~0.4-0.5. After incubation for 45 min at 37°C cells were harvested and washed three times with ice cold 10 % glycerol (11,300 *g*, 30 sec, 2°C). ~300 ng of Km cassette PCR-product was transformed via electroporation (1 mm cuvette, 1.8 kV, 25 µF, 200 Ω). After selection on kanamycin, gene deletions were confirmed via PCR using 'KO-Ver' primers (Supplementary Table 1). To remove the Km cassette, 50 mM L-rhamnose, which induces flippase gene expression, was added to an exponentially growing 2 ml LB culture at OD 0.5; induction time was ≥ 3 h at 30°C. Colonies were screened for kanamycin sensitivity and removal of antibiotic resistance cassette was confirmed by PCR (using 'KO-Ver' primers). For deletion of *icd*, 10 mM gluconate and 5 mM α-ketoglutarate was supplied to LB plates as well as to liquid cultures.

Gene overexpression

For the overexpression of the dihydrolipoamide dehydrogenase (*lpd*) (including an N-terminal 6x His-Tag) the corresponding gene was amplified from *E. coli* genomic DNA by PCR using primers lpd_A and lpd_D. The PCR product (lpd^{WT}) was cloned into pNivC vector. To clone the rationally designed *lpd* variants (which are specific to $NADP^+$), the mutations described by Bocanegra *et al.* were introduced by a fusion PCR of the PCR products generated with primer pairs lpd_A + lpd_B and lpd_C + lpd_D, resulting in the *lpd* variant lpd^{5M} (corresponding to Bocanegra's Mutant A: Glu203Val, Met204Arg, Phe205Lys, Asp206His, Pro210Arg). The PCR product was cloned into pNivC vector resulting in pNivC-lpd^{5M}. To generate pNivC-lpd^{7M} (corresponding to Bocanegra's Mutant C Glu203Val, Met204Arg, Phe205Lys, Asp206His, Pro210Arg, Gly185Ala, Gly189Ala) pNivC-lpd^{5M} was used as a PCR template, primers lpd_MutB-F and lpd_MutB-R were used together with pNiv-Amp-F and pNiv-Amp-R, respectively. The PCR products were fused by CPEC cloning[33] to generate pNivC-lpd^{7M}. The genes were cloned with *EcoR*I and *Pst*I (FastDigest, Thermo Scientific) into the expression vector pZ-ASM (p15A origin, Streptomycin resistance, medium strength promoter), generating pZ-ASM-lpd^{WT}, and pZ-ASM-lpd^{7M}.

NADP-dependent non-phosphorylating glyceraldehyde 3-phosphate dehydrogenase from *Streptococcus mutans* (gapN, UniProt: Q59931[21]) and engineered formate dehydrogenase from *Mycobacterium vaccae* (MVa-

3M-*fdh*[25]) were synthesized after codon adaptation for *E. coli*[34]. Recognition sites of restriction enzymes required for cloning were removed[35]. Gene synthesis was performed by Baseclear (Leiden, The Netherlands). Each gene was cloned with an N-terminal 6x His-Tag into a pNivC vector downstream of ribosome binding site "C" (AAGTTAAGAGGCAAGA)[35]. To generate pNivC-(MVa-4M-*fdh*), primers fdh-Mva-4M-F and fdh-Mva-4M-R were used together with pNiv-Amp-F and pNiv-Amp-R, respectively, on pNivC-(MVa-3M-*fdh*). The PCR products were combined by CPEC cloning[33]. Restriction enzymes *EcoR*I and *Pst*I (FastDigest, Thermo Scientific) were used to transfer the genes into the expression vector pZ-ASM (p15A origin, Streptomycin resistance, medium promoter) or pZ-ASS (p15A origin, Streptomycin resistance, strong promoter) for gapN, resulting in pZ-ASM-gapN and pZ-ASS-gapN. fdh^{4M} was cloned into pZ-ASM, pZ-ASS, and pZ-MSM (pMB1 origin, Streptomycin resistance, medium promoter)[18] resulting in pZ-ASM-fdh^{4M}, pZ-ASS-fdh^{4M}, and pZ-MSM-fdh^{4M}.

Media and growth conditions

LB medium (1% NaCl, 0.5% yeast extract, 1% tryptone) was used for growth during cloning and to generate gene deletions. When appropriate, antibiotics were used in following concentrations: kanamycin, 25 µg/mL; ampicillin, 100 µg/mL; streptomycin, 100 µg/mL; and chloramphenicol, 30 µg/mL. For deletion and maintenance of the *icd* deletion strain, 5 mM 2-ketoglutarate and 10 mM gluconate were added to LB plates. For growth experiments, M9 minimal media (50 mM Na_2HPO_4, 20 mM KH_2PO_4, 1 mM NaCl, 20 mM NH_4Cl, 2 mM $MgSO_4$ and 100 µM $CaCl_2$, 134 µM EDTA, 13 µM $FeCl_3 \cdot 6H_2O$, 6.2 µM $ZnCl_2$, 0.76 µM $CuCl_2 \cdot 2H_2O$, 0.42 µM $CoCl_2 \cdot 2H_2O$, 1.62 µM H_3BO_3, 0.081 µM $MnCl_2 \cdot 4H_2O$) was used.

Different carbon sources were used as described in the text, in concentrations that were scaled according to their energy of combustion. Specifically, glucose, with an energy of combustion of ~2910 kJ/mol[36], was set as 10 mM. The concentrations of the other carbon sources were scaled according to the ratio of their combustion energies[36] to that of glucose: glycerol, with ~1650 kJ/mol, was set to 10 X (2910/1650) = 18 mM; pyruvate, with ~1160 kJ/mol, was set to 25 mM; acetate, with ~850 kJ/mol, was set to 34 mM; succinate, with ~1540 kJ/mol, was set to 19 mM; xylose, with ~2440 kJ/mol, was set to 12 mM; gluconate, with ~2660 kJ/mol, was set to 11 mM.

Overnight cultures for growth experiments were incubated in 4 mL M9 medium containing 11 mM gluconate and 3 mM 2-ketoglutarate. Prior to inoculation, cultures were harvested by centrifugation (3,960 *g*, 3 min) and washed three times in M9 medium to clean cells from residual carbon sources. Growth experiments were inoculated to a starting OD_{600} of 0.01 and carried out in 96-well microtiter plates (Nunclon Delta Surface, Thermo Scientific) at 37°C. Each well contained 150 µL of culture and, to avoid evaporation, 50 µL mineral oil (Sigma-Aldrich). A plate reader (Infinite M200 pro, Tecan) was used for incubation, shaking and OD_{600} measurements (controlled by Tecan I-control v1.11.1.0). The cultivation program contained three cycles of 4 shaking phases, 1 min of each: linear shaking, orbital shaking at an amplitude of 3 mm, linear shaking, and orbital shaking at an amplitude of 2 mm. After each round of shaking (~12.5 min), absorbance (OD 600 nm) was measured in each well. Raw data from the plate reader were calibrated to cuvette values according to $OD_{cuvette}=OD_{plate}/0.23$. Growth curves were plotted in MATLAB and represent averages of triplicate measurements; in all cases, variability between triplicate measurements was less than 5%.

ORCID

Arren Bar-Even: 0000-0002-1039-4328

Steffen Lindner: 0000-0003-3226-3043

Oren Yishai: 0000-0001-8712-3959

Sophia Belkhelfa: 0000-0001-5943-4442

Madeleine Bouzon: 0000-0002-9581-6584

Volker Döring: 0000-0002-9453-6572

Acknowledgements

The authors thank Nico Claassens for critical reading of the manuscript. This work was funded by the Max Planck Society.

References

(1) Kabus, A.; Georgi, T.; Wendisch, V. F.; Bott, M. (2007) Expression of the Escherichia coli pntAB genes encoding a membrane-bound transhydrogenase in Corynebacterium glutamicum improves L-lysine formation, *Appl Microbiol Biotechnol 75*, 47-53.

(2) Blombach, B.; Schreiner, M. E.; Bartek, T.; Oldiges, M.; Eikmanns, B. J. (2008) Corynebacterium glutamicum tailored for high-yield L-valine production, *Appl Microbiol Biotechnol 79*, 471-9.

(3) Park, S. H.; Kim, H. U.; Kim, T. Y.; Park, J. S.; Kim, S. S.; Lee, S. Y. (2014) Metabolic engineering of Corynebacterium glutamicum for L-arginine production, *Nature communications 5*, 4618.

(4) Kim, S. Y.; Lee, J.; Lee, S. Y. (2015) Metabolic engineering of Corynebacterium glutamicum for the production of L-ornithine, *Biotechnol Bioeng 112*, 416-21.

(5) Wang, Y.; San, K. Y.; Bennett, G. N. (2013) Improvement of NADPH bioavailability in Escherichia coli through the use of phosphofructokinase deficient strains, *Appl Microbiol Biotechnol 97*, 6883-93.

(6) Ng, C. Y.; Farasat, I.; Maranas, C. D.; Salis, H. M. (2015) Rational design of a synthetic Entner-Doudoroff pathway for improved and controllable NADPH regeneration, *Metab Eng 29*, 86-96.

(7) Spaans, S. K.; Weusthuis, R. A.; van der Oost, J.; Kengen, S. W. (2015) NADPH-generating systems in bacteria and archaea, *Frontiers in microbiology 6*, 742.

(8) Lee, W. H.; Kim, M. D.; Jin, Y. S.; Seo, J. H. (2013) Engineering of NADPH regenerators in Escherichia coli for enhanced biotransformation, *Appl Microbiol Biotechnol 97*, 2761-72.

(9) Aslan, S.; Noor, E.; Bar-Even, A. (2017) Holistic bioengineering: rewiring central metabolism for enhanced bioproduction, *Biochem J 474*, 3935-3950.

(10) Zhang, L.; King, E.; Luo, R.; Li, H. (2018) Development of a High-Throughput, In Vivo Selection Platform for NADPH-Dependent Reactions Based on Redox Balance Principles, *ACS synthetic biology 7*, 1715-1721.

(11) van der Donk, W. A.; Zhao, H. (2003) Recent developments in pyridine nucleotide regeneration, *Curr Opin Biotechnol 14*, 421-6.

(12) Tishkov, V. I.; Popov, V. O. (2006) Protein engineering of formate dehydrogenase, *Biomol Eng 23*, 89-110.

(13) Johannes, T. W.; Woodyer, R. D.; Zhao, H. (2007) Efficient regeneration of NADPH using an engineered phosphite dehydrogenase, *Biotechnology and Bioengineering 96*, 18.

(14) Sauer, U.; Canonaco, F.; Heri, S.; Perrenoud, A.; Fischer, E. (2004) The soluble and membrane-bound transhydrogenases UdhA and PntAB have divergent functions in NADPH metabolism of Escherichia coli, *J Biol Chem 279*, 6613-9.

(15) Kabir, M. M.; Shimizu, K. (2004) Metabolic regulation analysis of icd-gene knockout Escherichia coli based on 2D electrophoresis with MALDI-TOF mass spectrometry and enzyme activity measurements, *Appl Microbiol Biotechnol 65*, 84-96.

(16) Bocanegra, J. A.; Scrutton, N. S.; Perham, R. N. (1993) Creation of an NADP-dependent pyruvate dehydrogenase multienzyme complex by protein engineering, *Biochemistry 32*, 2737-40.

(17) Bar-Even, A.; Noor, E.; Savir, Y.; Liebermeister, W.; Davidi, D.; Tawfik, D. S.; Milo, R. (2011) The moderately efficient enzyme: evolutionary and physicochemical trends shaping enzyme parameters, *Biochemistry 50*, 4402-10.

(18) Braatsch, S.; Helmark, S.; Kranz, H.; Koebmann, B.; Jensen, P. R. (2008) Escherichia coli strains with promoter libraries constructed by Red/ET recombination pave the way for transcriptional fine-tuning, *Biotechniques 45*, 335-7.

(19) Wenk, S.; Yishai, O.; Lindner, S. N.; Bar-Even, A. (2018) An Engineering Approach for Rewiring Microbial Metabolism, *Methods Enzymol 608*, 329-367.

(20) Fischer, E.; Sauer, U. (2003) A novel metabolic cycle catalyzes glucose oxidation and anaplerosis in hungry Escherichia coli, *J Biol Chem 278*, 46446-51.

(21) Cobessi, D.; Tete-Favier, F.; Marchal, S.; Azza, S.; Branlant, G.; Aubry, A. (1999) Apo and holo crystal structures of an NADP-dependent aldehyde dehydrogenase from Streptococcus mutans, *J Mol Biol 290*, 161-73.

(22) Takeno, S.; Murata, R.; Kobayashi, R.; Mitsuhashi, S.; Ikeda, M. (2010) Engineering of Corynebacterium glutamicum with an NADPH-generating glycolytic pathway for L-lysine production, *Appl Environ Microbiol 76*, 7154-60.

(23) Marchal, S.; Rahuel-Clermont, S.; Branlant, G. (2000) Role of glutamate-268 in the catalytic mechanism of nonphosphorylating glyceraldehyde-3-phosphate dehydrogenase from Streptococcus mutans, *Biochemistry 39*, 3327-35.

(24) Sauer, U.; Eikmanns, B. J. (2005) The PEP-pyruvate-oxaloacetate node as the switch point for carbon flux distribution in bacteria, *FEMS Microbiol Rev 29*, 765-94.

(25) Hoelsch, K.; Suhrer, I.; Heusel, M.; Weuster-Botz, D. (2013) Engineering of formate dehydrogenase: synergistic effect of mutations affecting cofactor specificity and chemical stability, *Appl Microbiol Biotechnol 97*, 2473-81.

(26) Falke, D.; Schulz, K.; Doberenz, C.; Beyer, L.; Lilie, H.; Thiemer, B.; Sawers, R. G. (2010) Unexpected oligomeric structure of the FocA formate channel of Escherichia coli : a paradigm for the formate-nitrite transporter family of integral membrane proteins, *FEMS Microbiol Lett 303*, 69-75.
(27) Haverkorn van Rijsewijk, B. R.; Kochanowski, K.; Heinemann, M.; Sauer, U. (2016) Distinct transcriptional regulation of the two Escherichia coli transhydrogenases PntAB and UdhA, *Microbiology 162*, 1672-1679.
(28) Yishai, O.; Lindner, S. N.; Gonzalez de la Cruz, J.; Tenenboim, H.; Bar-Even, A. (2016) The formate bio-economy, *Curr Opin Chem Biol 35*, 1-9.
(29) Yishai, O.; Bouzon, M.; Doring, V.; Bar-Even, A. (2018) In Vivo Assimilation of One-Carbon via a Synthetic Reductive Glycine Pathway in Escherichia coli, *ACS synthetic biology*.
(30) Jensen, S. I.; Lennen, R. M.; Herrgard, M. J.; Nielsen, A. T. (2015) Seven gene deletions in seven days: Fast generation of Escherichia coli strains tolerant to acetate and osmotic stress, *Scientific reports 5*, 17874.
(31) Thomason, L. C.; Costantino, N.; Court, D. L. (2007) E. coli genome manipulation by P1 transduction, *Curr Protoc Mol Biol Chapter 1*, Unit 1 17.
(32) Baba, T.; Ara, T.; Hasegawa, M.; Takai, Y.; Okumura, Y.; Baba, M.; Datsenko, K. A.; Tomita, M.; Wanner, B. L.; Mori, H. (2006) Construction of Escherichia coli K-12 in-frame, single-gene knockout mutants: the Keio collection, *Mol Syst Biol 2*, 2006-2008.
(33) Quan, J.; Tian, J. (2014) Circular polymerase extension cloning, *Methods Mol Biol 1116*, 103-17.
(34) Grote, A.; Hiller, K.; Scheer, M.; Munch, R.; Nortemann, B.; Hempel, D. C.; Jahn, D. (2005) JCat: a novel tool to adapt codon usage of a target gene to its potential expression host, *Nucleic Acids Res 33*, W526-31.
(35) Zelcbuch, L.; Antonovsky, N.; Bar-Even, A.; Levin-Karp, A.; Barenholz, U.; Dayagi, M.; Liebermeister, W.; Flamholz, A.; Noor, E.; Amram, S.; Brandis, A.; Bareia, T.; Yofe, I.; Jubran, H.; Milo, R. (2013) Spanning high-dimensional expression space using ribosome-binding site combinatorics, *Nucleic Acids Res 41*, e98.
(36) Flamholz, A.; Noor, E.; Bar-Even, A.; Milo, R. (2012) eQuilibrator--the biochemical thermodynamics calculator, *Nucleic Acids Res 40*, D770-5.

Tables

Table 1. Strains and plasmids used in this study

name	Use/deletion	References
DH5α	Cloning of overexpression constructs	
SIJ488	WT	[30]
JW1122	icd::kan knockout Keio collection	[32]
ΔZ	Δzwf	This study
ΔZM	Δzwf ΔmaeA	This study
ΔZMP	Δzwf ΔmaeA ΔpntAB	This study
ΔZMS	Δzwf ΔmaeA ΔsthA	This study
ΔZMPS	Δzwf ΔmaeA ΔpntAB ΔsthA	This study
ΔZMPI	Δzwf ΔmaeA ΔpntAB Δicd::kan	This study
ΔZMSI	Δzwf ΔmaeA ΔsthA Δicd::kan	This study
ΔZMPSI (NADPHaux)	Δzwf ΔmaeA ΔpntAB ΔsthA Δicd::kan	This study
ΔZMPSIEE	Δzwf ΔmaeA ΔpntAB ΔsthA Δicd Δedd-eda	This study
pZ-ASM	Over-expression plasmid with p15A origin (medium copy number), Streptomycin resistance, constitutive strong promoter (5'-ACCTATTGACAATTAAAGGCTAAAATGCTATAATTCCAC-3')	[19]
pZ-ASS	Over-expression plasmid with p15A origin (medium copy number), Streptomycin resistance, constitutive strong promoter (5'-AATACTTGACATATCACTGTGATTCACATATAATATGCG-3')	[19]
pZ-MSM	Over-expression plasmid with pMB1 origin (high copy number), Streptomycin resistance, constitutive medium strength promoter (5'-ACCTATTGACAATTAAAGGCTAAAATGCTATAATTCCAC-3')	[19]
pZ-ASM-lpd^{WT}	pZ-ASM backbone for overexpression of *E. coli* wildtype *lpd*	This study
pZ-ASM-lpd^{7M}	pZ-ASM backbone for overexpression of *E. coli lpd*^{7M} (E203V, M204R, F205K, D206H, P210R, G185A, G189A)	This study
pZ-ASM-gapN	pZ-ASM backbone for overexpression of *gapN* from *S. mutans*	This study
pZ-ASS-gapN	pZ-ASS backbone for overexpression of *gapN* from *S. mutans*	This study
pZ-ASM-MVfdh^{4M}	pZ-ASM backbone for overexpression of engineered *fdh* from *M. vaccae* (C145S/A198G/D221Q/C255V)	This study
pZ-ASS-MVfdh^{4M}	pZ-ASS backbone for overexpression of engineered *fdh* from *M. vaccae* (C145S/A198G/D221Q/C255V)	This study
pZ-MSM-MVfdh^{4M}	pZ-MSM backbone for overexpression of engineered *fdh* from *M. vaccae* (C145S/A198G/D221Q/C255V)	This study

Figure Legends

Figure 1

Schematic representation of the NADPH auxotrophic *E. coli*. Enzymes producing NADPH are shown in blue arrows. Deleted enzymes are indicated using a red crossing line. Carbon sources are shown in green. Once isocitrate dehydrogenase (Icd) is disrupted, 2-ketoglutarate is added to the medium as a source of glutamate and related amino-acids. The membrane-bound transhydrogenase (PntAB) is schematically shown with the proton translocated across the membrane to energize the unfavorable electron transfer. The soluble transhydrogenase (SthA) is disrupted to avoid depletion of the NADPH pool (see main text). Abbreviations: G6P – glucose 6-phosphate; 6PG – 6-phosphogluconate; Ru5P – ribulose 5-phosphate; F6P – fructose 6-phosphate; GAP – glyceraldehyde 3-phosphate; Pyr – pyruvate; AcCoA – acetyl-CoA; ICit – isocitrate; 2KG – 2-ketoglutarate; Suc – succinate; Mal – malate.

Figure 2

Construction of the NADPH auxotroph strain. Growth phenotypes of intermediate gene deletion strains are shown using multiple carbon sources. Concentrations of the carbon sources were normalized to the energy of combustion of different growth substrates. All growth experiments were performed in triplicates, which in all cases resulted in identical curves (± 5%), indicating that no mutation occurred to enable the observed growth. The growth curves of the WT, ΔZ, ΔZM, and ΔZMS strains on all carbon sources were identical and hence are shown on the same graph.

Figure 3

Maximal OD of the NADPHaux strain scales with the concentration of gluconate as sole source of NADPH. Different carbon sources present a similar trend. Concentrations of the carbon sources were normalized according to the combustion energy of the compounds, as described in the Methods section. In all cases, 3 mM of 2-ketoglutarate was added. All growth experiments were performed in triplicates, which in all cases resulted in identical curves (± 5%), indicating that no mutation occurred to enable the observed growth.

Figure 4

Overexpression of engineered dihydrolipoamide dehydrogenase (*lpd*^{7M}) that accepts $NADP^+$ restores growth on all carbon sources. The engineered enzyme, harboring 7 mutations[16], is marked as lpd^{7M}. Overexpression of non-mutated lpd, marked as lpd^{WT}, did not rescue growth. Both enzymes were expressed from a medium copy number plasmid and under the regulation of a medium strength promoter. In all cases, 3 mM of 2-ketoglutarate was added. All growth experiments were performed in triplicates, which in all cases resulted in identical curves (± 5%), indicating that no mutation occurred to enable the observed growth.

Figure 5

Overexpression of NADP-dependent non-phosphorylating glyceraldehyde 3-phosphate dehydrogenase of *Streptococcus mutans* (GapN) rescues the growth on the NADPHaux strain. (A) Growth on different carbon sources is restored upon expression of GapN from a medium copy number plasmid and under the regulation of

a strong promoter (gluconate not added). In all cases, 3 mM of 2-ketoglutarate was added. All growth experiments were performed in triplicates, which in all cases resulted in identical curves (± 5%), indicating that no mutation occurred to enable the observed growth. (B) Schematic representation of a cyclic flux when the cell is fed with carbon sources that enter 'lower metabolism' (pyruvate, succinate, acetate). This cycle transfer electrons from NADH to NADPH at the expense of ATP hydrolysis.

Figure 6

Addition of formate rescues the growth of the NADPHaux strain expressing engineered formate dehydrogenase. Engineered formate dehydrogenase from *Mycobacterium vaccae* N10, carrying 4 mutations (fdh^{4M}), with high specificity towards the reduction of $NADP^+$, was overexpressed from a high copy number plasmid and under the regulation of a medium strength promoter. Glycerol (18 mM) served as carbon source and 3 mM of 2-ketoglutarate was added. All growth experiments were performed in triplicates, which in all cases resulted in identical curves (± 5%), indicating that no mutation occurred to enable the observed growth.

Figure 7

Addition of cinnamyl alcohol rescues the growth of the NADPHaux strain. Glycerol (18 mM) served as carbon source and 3 mM of 2-ketoglutarate was added. All growth experiments were performed in triplicates, which in all cases resulted in identical curves (± 5%), indicating that no mutation occurred to enable the observed growth.

Figure 1

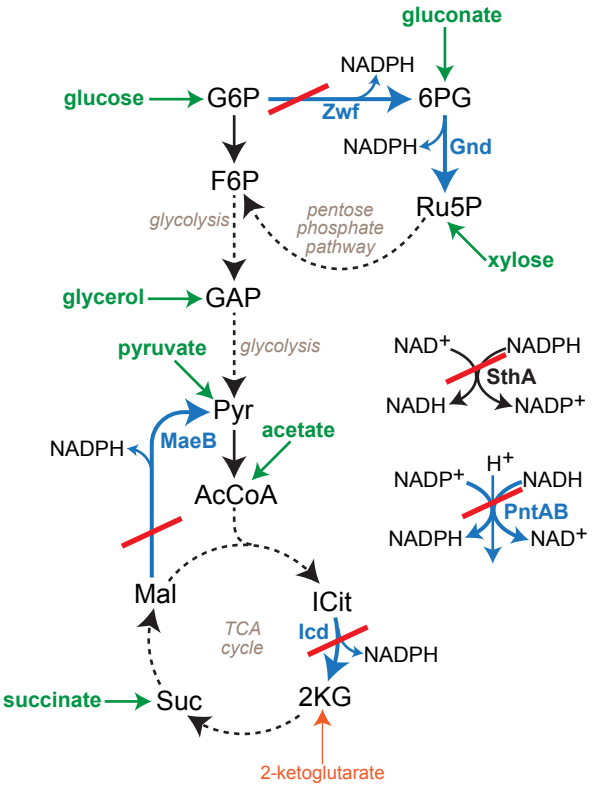
gluconate
NADPH
glucose
G6P
Zwf
6PG
NADPH
Gnd
F6P
glycolysis
pentose phosphate pathway
Ru5P
xylose
glycerol
GAP
pyruvate
glycolysis
NAD+
NADPH
SthA
NADH
NADP+
Pyr
NADPH
MaeB
acetate
AcCoA
NADP+
H+
NADH
PntAB
NADPH
NAD+
Mal
ICit
TCA cycle
Icd
NADPH
succinate
Suc
2KG
2-ketoglutarate

Figure 2

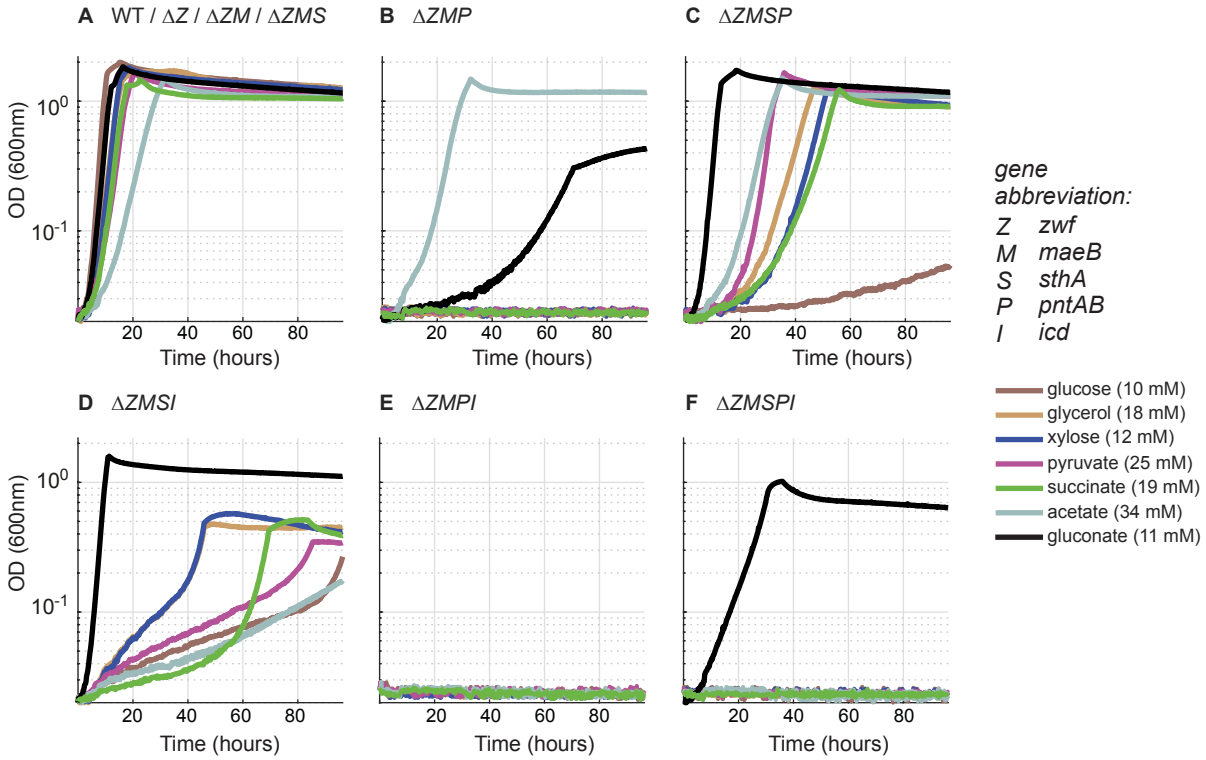
A WT / ΔZ / ΔZM / ΔZMS
B ΔZMP
C ΔZMSP
D ΔZMSI
E ΔZMPI
F ΔZMSPI
OD (600nm)
Time (hours)
gene abbreviation:
Z zwf
M maeB
S sthA
P pntAB
I icd
glucose (10 mM)
glycerol (18 mM)
xylose (12 mM)
pyruvate (25 mM)
succinate (19 mM)
acetate (34 mM)
gluconate (11 mM)

Figure 3

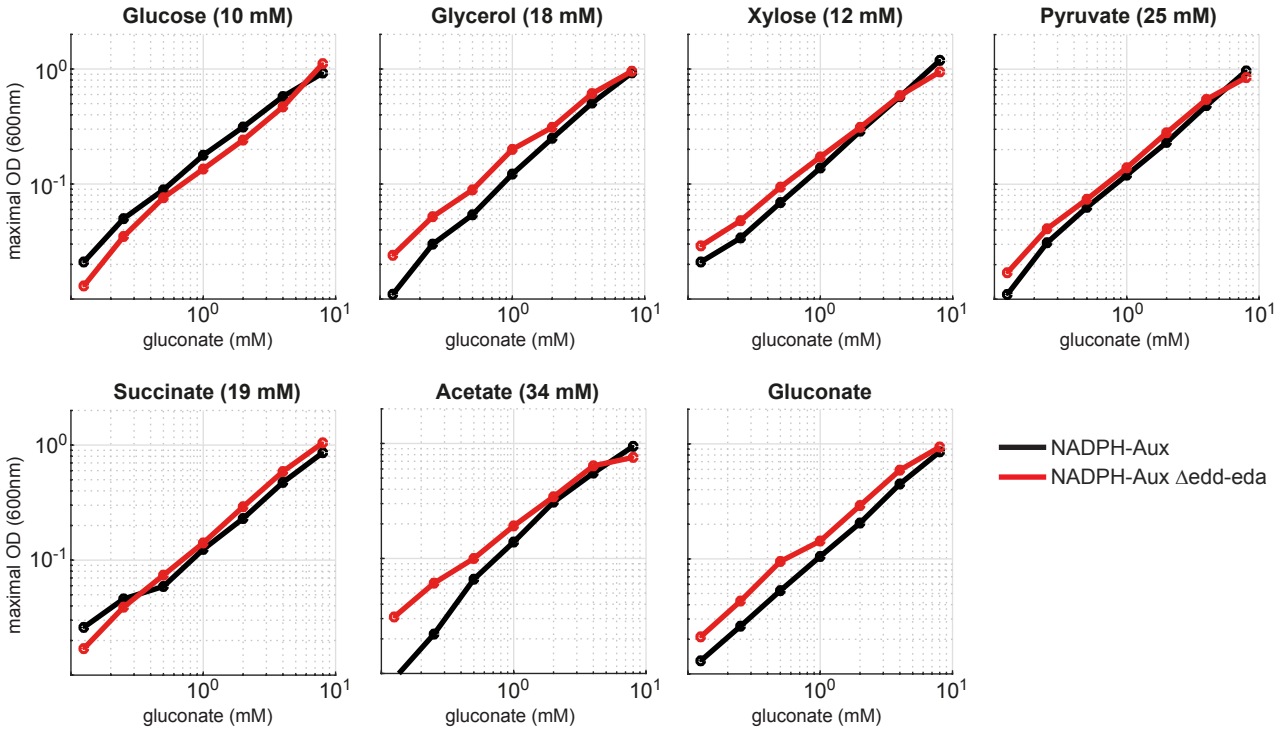
Glucose (10 mM)
Glycerol (18 mM)
Xylose (12 mM)
Pyruvate (25 mM)
Succinate (19 mM)
Acetate (34 mM)
Gluconate
maximal OD (600nm)
gluconate (mM)
NADPH-Aux
NADPH-Aux Δedd-eda

Figure 4

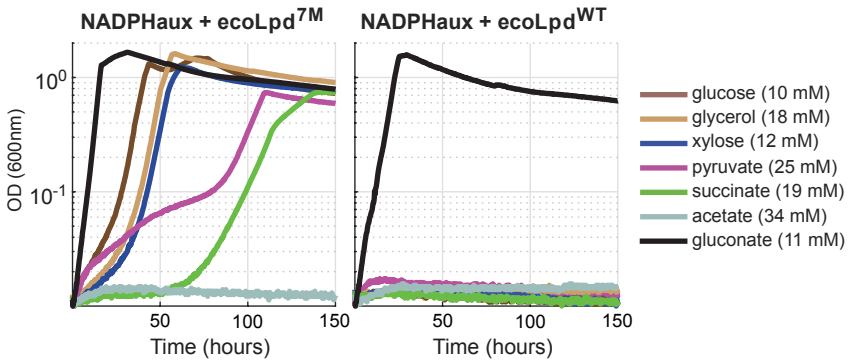
NADPHaux + ecoLpd7M
NADPHaux + ecoLpdWT
OD (600nm)
10^0
10^-1
50
100
150
Time (hours)
glucose (10 mM)
glycerol (18 mM)
xylose (12 mM)
pyruvate (25 mM)
succinate (19 mM)
acetate (34 mM)
gluconate (11 mM)

Figure 5

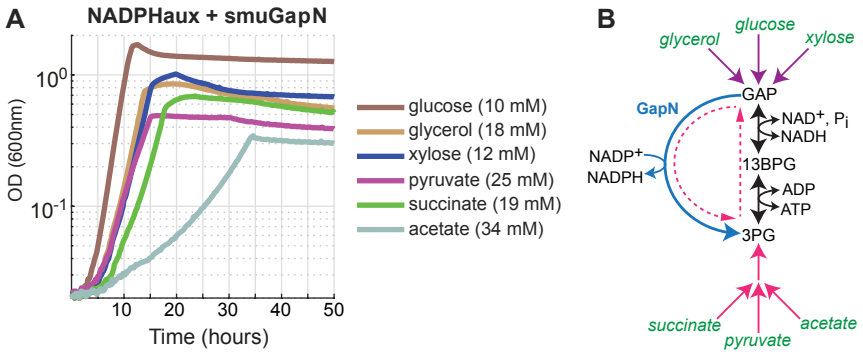
A
NADPHaux + smuGapN
OD (600nm)
10^0
10^{-1}
10
20
30
40
50
Time (hours)
glucose (10 mM)
glycerol (18 mM)
xylose (12 mM)
pyruvate (25 mM)
succinate (19 mM)
acetate (34 mM)
B
glycerol
glucose
xylose
GAP
GapN
NAD^+, P_i
NADH
$NADP^+$
NADPH
13BPG
ADP
ATP
3PG
succinate
pyruvate
acetate

Figure 6

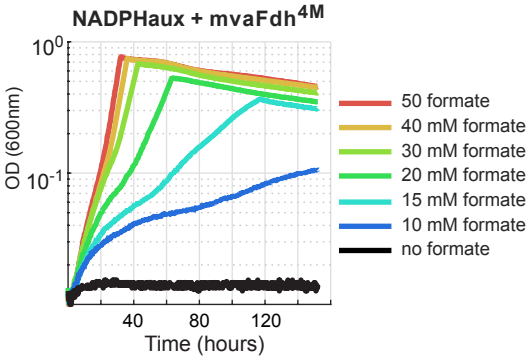
NADPHaux + mvaFdh4M
10^0
10^-1
OD (600nm)
40
80
120
Time (hours)
50 formate
40 mM formate
30 mM formate
20 mM formate
15 mM formate
10 mM formate
no formate

Figure 7

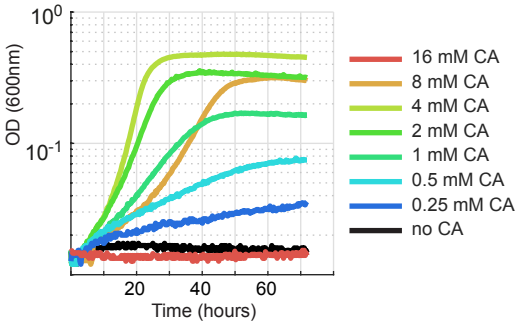
10^0
10^{-1}
OD (600nm)
20
40
60
Time (hours)
16 mM CA
8 mM CA
4 mM CA
2 mM CA
1 mM CA
0.5 mM CA
0.25 mM CA
no CA

Table of Contents Graphic